Advances in Materials
2025, Vol. 14, No. 2, pp. 36-45
https://doi.org/10.11648/j.am.20251402.11

Research Article

Thermomechanical Characterization and Numerical Modeling of Thermal Transfer of Plaster-based Insulating Composite Materials with Gradual Typha Contents

El Hadji Abdoul Aziz Cisse*, Papa Touty Traore, Seydou Faye, Moussa Dieng, Mor Ndiaye, Issa Diagne

Department of Physics, Semiconductor Laboratory, Cheikh Anta Diop University of Dakar, Dakar, Senegal

Abstract

The building and construction sectors are responsible for 39% of global greenhouse gas emissions, but they are among the largest consumers of energy. If all indicators show that demand would be exponential in the future. Decarbonization and reduction of energy consumption in buildings are urgent for environmental preservation and resilience to extreme temperature increases. This article aims to present environmentally friendly bio-sourced insulation as a more sustainable circular economy strategy. However, we present the results of thermal and mechanical characterization of plaster samples with the addition of typha fibers in different proportions. Thus, after having carried out the mechanical traction and compression tests by the press, a thermophysical characterization by the asymmetric hot plane method allowed us to have the conductivity and thermal effusivity of the different samples of plaster binder with 0%, 5%, 10%, 15% and 20% in typha. With these data, we modeled the heat transfer phenomena in a flat wall based on plaster-typha. A numerical resolution of the heat equation by the finite difference method is applied to this model along one dimension. After simulating the calculation code, the results obtained made it possible to know the evolution of the temperature as a function of time and the depth of the wall. In addition, the influence of the exchange coefficients was highlighted on both sides, in order to know the optimal thermal insulation thickness of each sample.

Keywords

Characterization, Thermomechanics, Conductivity, Effusivity, Traction, Compression, Numerical Modeling, Typha-plaster and Exchange Coefficients

1. Introduction

Energy is, like food and water, an essential source for humanity. Today, global electricity consumption linked to the use of buildings represents nearly 55% of global electricity consumption [1]. This consumption could increase significantly in the future. The cause of this increase is due to demographics, gross domestic product (GDP) and the temperatures looming on the horizon. As part of decarbonization, the building and construction sector is increasingly adopting bio-sourced insulation from renewable and environmentally friendly resources [2-4]. Thus, thermal comfort drastically reduces energy demand, but with the use of bio-sourced materials which is a lever for the decarbonization of the built sector [5-7]. Those who are pushing many

*Corresponding author: elhadjiabdoulazizcisse1@gmail.com (El Hadji Abdoul Aziz Cisse)

Received: 18 March 2025; **Accepted:** 2 April 2025; **Published:** 29 April 2025

researchers are turning their research towards the valorization of our plant biomasses with the aim of isolating at low cost while preserving the environment [8-10]. We can note several studies carried out in this area: kapok plaster and plaster fiber [11], kapok, coconut, peanut shell fiber and rattan [12], typha clay [13], lime recovered in cement and typha concretes [14]. Through these numerous studies carried out on bio-sourced materials, to my knowledge, we have not yet seen a complete study on typha. That is to say from thermo-mechanical characterization to determinations of the optimal thermal insulation thickness of each test sample. In addition, typha is very present in many sites in Senegal [15]. This is why we see the originality of this work which is the subject of this research. To do this work better, we will structure it in three parts. In the first part, we will present the experimental process and the thermomechanical characterization. Second and third, we will respectively have the numerical modeling, the results and the discussions.

2. Experimental Process and Thermechanical Characterization

2.1. Experimental Process

In Senegal, Typha occurs in many sites: in the river valley, at Lake Guiers, in the Dakar techno-pole, etc. Figure 1 represents a photo of Typha in an aquatic environment. The molds used and the Typha grinding were developed in our previous work [15]. The drying time is 3 months in the shade of the laboratory with a temperature varying between 20 and 30 ℃. And the presence of water in these samples was determined by the ratio below.m_e=0,6× m_p with m_P=mass of plaster m_e= mass of water.

(a) (b)

Figure 1. *Typha aquatic environment (a), dried typha (b).*

Samples for thermal and mechanical testing are in Figure 2 below.

(a) (b)

Figure 2. *Thermal (a) and mechanical (b) samples.*

2.2. Thermomechanical Characterization

Thermomechanical characterization (thermal and mechanical) allows us to know the thermophysical and mechanical properties of materials before their use. The thermal characterization procedures using the asymmetric hot plane method and press mechanics were presented in our previous work [15].

3. Digital Modeling

3.1. Physical Model

This figure below represents a flat wall based on plaster-typha with its following simplifying assumptions:

1) Heat flow is unidirectional (following ox)
2) The thermal conductivities of materials are constants (λ=constant)
3) Thermal diffusivities are constants (α=constant)
4) TF1: front panel temperature = 300 K
5) TF2: rear surface temperature = 290 K
6) Ti: material temperature = 293 K

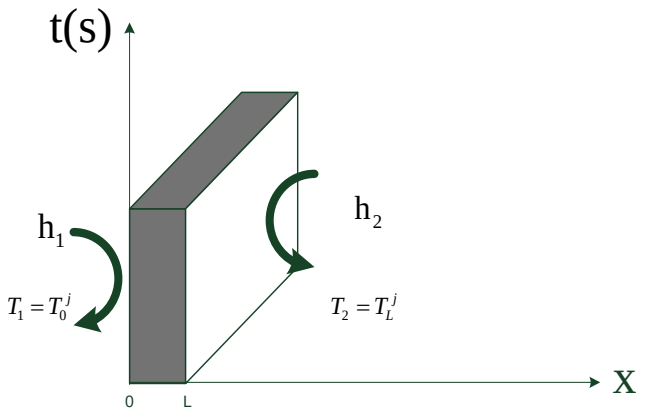

Figure 3. *Flat wall based on plaster-typha thermal insulation material.*

3.2. Mathematics Model

Below is the heat equation, which will be applied in the physical model of different plaster binder composites with gradual typha contents of 5%, 10%, 15% and 20%.

$$\frac{\partial^2 T(x,t)}{\partial^2 x} - \frac{1}{\alpha}\frac{\partial T(x,t)}{\partial t} = 0 \quad (1)$$

$$\text{With } \alpha = \frac{\lambda}{\rho C} \quad (2)$$

Equation (2) reflects the thermal diffusivity of each case of assumed uniform material.

$$\begin{cases} \lambda = \text{thermal conductivity} \\ \rho = \text{density} \\ C = \text{specific heat} \end{cases}$$

Equations (3) and (4) translate the conservation of the heat flow at the surface of the material of each case and their boundary conditions and equation (5) their initial condition.

$$h_1(T(0,t)-T_{f1}) = \lambda \frac{\partial T(x,t)}{\partial t}\Big|_{x=0} \quad (3)$$

$$h_2(T(L,t)-T_{f2}) = \lambda \frac{\partial T(x,t)}{\partial t}\Big|_{x=L} \quad (4)$$

$$T(x,0) = T^0 \quad (5)$$

We discretize the space into M nodes (figure 1a) and the time into N nodes (figure 1b).

The step of space Δx in the direction (ox) and that of time Δt. The steps are constant. T_i^j est la température au nœud i à la date j.

$$X_i = (i-1)\Delta x \quad (6)$$

$$t_j = (j-1)\Delta t \quad (7)$$

The index i identifies the variable x and the index j identifies the variable t. We make the following considerations:

$$dT \approx \Delta t \quad (8)$$

$$dx \approx \Delta x \quad (9)$$

$$dT \approx T_i^j - T_{i-1}^j \approx T_{i+1}^j - T_i^j \quad (10)$$

$$d^2T \approx (T_{i+1}^j - T_i^j) - (T_i^j - T_{i-1}^j) \quad (11)$$

$$= T_{i-1}^j - 2T_i^j + T_{i+1}^j$$

Taking into account equations (8), (9), (10) and (11), the different parts of equation (1) are given by equations (12) and (13).

$$\frac{\partial^2 T(x,t)}{\partial x^2} \approx \alpha \frac{T_{i-1}^j - 2T_i^j + T_{i+1}^j}{\Delta x^2} \quad (12)$$

$$\frac{\partial T(x,t)}{\partial t} \approx \frac{T_i^{j+1} - T_i^j}{\Delta t} \quad (13)$$

Taking into account equations (12) and (13), equation (1) of heat is translated by equation (14).

$$T_i^{j+1} = (1-2P)T_i^j + PT_{i+1}^j + PT_{i-1}^j \quad (14)$$

The expression for P, corresponding to the Fourier number, is given by relation (15) and relation (16) is.

The stability condition of the algorithm.

$$P = \alpha \frac{\Delta t}{\Delta x^2} \quad (15)$$

$$\Delta t \prec \frac{\Delta x^2}{2\alpha} \quad (16)$$

4. Numerical Solving

The application of the finite difference method is represented in figure 4 by a mesh of the material.

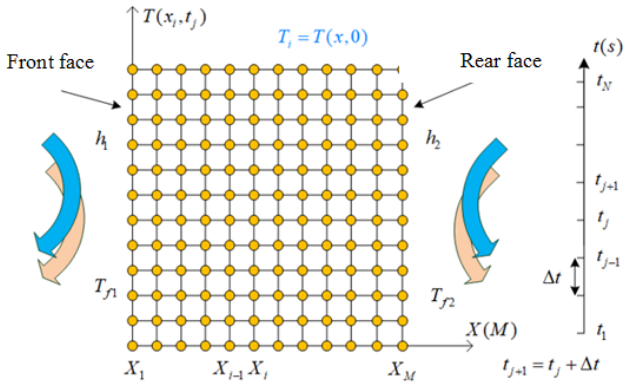

Figure 4. *Material mesh.*

To discretize the boundary conditions, we add two fictitious nodes: i=0 and i=M+1. At point i=1, we consider the fictitious node i=0 and at point i=M, we consider the fictitious node M+1. Boundary conditions (3) and (4) become (17) and (18), equation (19) defines the initial condition for each case.

$$\lambda \frac{\partial T(x,t)}{\partial x}\Big|_{x=0} = \lambda \frac{T_2^j - T_0^j}{2\Delta x} = h_{1x}(T_1^j - T_{f1}) \quad (17)$$

$$-\lambda \frac{\partial T(x,t)}{\partial x}\Big|_{x=L} = -\lambda \frac{T_{M+1}^j - T_{M-1}^j}{2\Delta x} = h_{2x}(T_M^j - T_{f2}) \quad (18)$$

$$T(x,0) = T_i^1 \quad (19)$$

Equations (17) and (18) give equations (20) and (21) respectively.

$$T_0^j = -2\frac{h_1\Delta x}{\lambda}(T_1^j - T_{f1}) + T_2^j \quad (20)$$

$$T_{M+1}^j = -2\frac{h_2\Delta x}{\lambda}(T_M^j - T_{f2}) + T_{M-1}^j \quad (21)$$

With the fictitious nodes i=0 and i=M+1, equation (14) allows us to obtain equations (22) and (23):

$$T_1^{j+1} = (1-2P)T_1^j + PT_2^j + PT_0^j \quad (22)$$

$$T_M^{j+1} = (1-2P)T_M^j + PT_{M+1}^j + PT_{M-1}^j \quad (23)$$

By replacing in equations (22) and (23) respectively the expressions of (equation 20) and (equation 21), we obtain expressions (24) and (25).

$$T_1^{j+1} = \left[(1-2P) - \frac{2Ph_1\Delta x}{\lambda}\right]T_1^j + 2PT_2^j + \frac{2Ph_1\Delta x}{\lambda}T_{f1} \quad (24)$$

$$T_M^{j+1} = \left[(1-2P) - \frac{2Ph_2\Delta x}{\lambda}\right]T_M^j + 2PT_{M-1}^j + \frac{2Ph_2\Delta x}{\lambda}T_{f2} \quad (25)$$

$$\text{Avec } A = \left[(1-2P) - \frac{2Ph_1\Delta x}{\lambda}\right] \quad (26)$$

$$B = \left[(1-2P) - \frac{2Ph_2\Delta x}{\lambda}\right] \quad (27)$$

$$C = \frac{2Ph_1\Delta x}{\lambda} \quad (28)$$

$$D = \frac{2Ph_2\Delta x}{\lambda} \quad (29)$$

h_1 et h_2 are constants hence the boundary conditions at point i=1 and i=M taking into account the parameters α, A, B, C et D.

$$T_1^{j+1} = AT_1^j + 2PT_2^j + CT_{f1} \quad (30)$$

$$T_M^{j+1} = BT_M^j + 2PT_{M-1}^j + DT_{f2} \quad (31)$$

$$T_i^j = T^0 \quad (32)$$

The expressions for the temperature and the flux density are given respectively by relations (33) and (34) considering the given boundary and initial conditions (equations 30, 31 and 32).

$$T_i^{j+1} = (1-2P)T_i^j + PT_{i+1}^j + PT_{i-1}^j \quad (33)$$

with $2 \le i \le M$ et $1 \le j \le N-1$

$$\Phi_i^j(\alpha, h_1, h_2) = \frac{-\lambda\left[T_{i+1}^j(\alpha, h_1, h_2) - T_i^j(\alpha, h_1, h_2)\right]}{\Delta x} \quad (34)$$

with $1 \le i \le M-1$ et $1 \le j \le N$

The numerical resolution of the equations was done by a finite difference method. The following will present these results, followed by discussions.

5. Results and Discussions

5.1. Results and Discussions of Thermomechanical Characterization

5.1.1. Thermal Characterization Results and Discussions

The tables below represent the thermophysical and mechanical results from the asymmetric hot plane method and the mechanical press test. The thermophysical characterization results are presented in the Table 1.

Table 1. *Thermal characterization results.*

Sample Typha plaster (0%, 5%, 10%, 15% et 20%)	**E0**	**E5**	**E10**	**E15**	**E20**
Mass of dry samples in g	274,67	224,29	183,59	135,33	131,9
Thermal conductivity in W/m.K	0,6795	0,1743	0,1554	0,1378	0,0652
Thermal effusivity in J/.m^2.K.$s^{1/2}$	1022,4	560,9213	486,3481	447,8512	276,132
Thermal diffusivity	4,4171 10^{-7}	9,65586 10^{-8}	1,02096 10^{-7}	9,4674 10^{-8}	5,57522 10^{-8}
Density kg/m^3	1373,35	1121,45	917,95	676,65	659,5

Table 1 shows the results of the thermal characterization, while Table 2 shows the results of the mechanical characterization.

5.1.2. Results and Discussions of Mechanical Characterization

Table 2 shows the results obtained by mechanical testing.

Table 2. *Mechanical test results.*

Mass Typha Plaster percentage			**E0**	**E5**	**E10**	**E15**	**E20**
Traction		Force en KN	1,855	1,845	1,466	1,126	0,632
		Pressure in MPa	0,412	0,410	0,326	0,250	0,141
Compression	C1	Force en KN	17,372	8,836	7,556	6,991	3,152
		Pressure in MPa	0,772	0,393	0,336	0,311	0,140
	C2	Force in KN	17,749	10,282	7,891	6,912	3,965
		Pressure in MPa	0,789	0,457	0,339	0,307	0,176
	$C_{moyenne}$	Force en KN	17,5605	9,559	7,7235	6,9515	3,5585
		Pression en MPa	0,7805	0,425	0,3375	0,309	0,158
Masse in Kg			320,05	279,30	257,15	198,97	135
Density Kg/m^3			1250,195	1091,016	1004,492	777,226	527,344

Tables 1 and 2 show the thermophysical and mechanical results. We found that as the mass percentage of typha increases in the matrices, the thermophysical and mechanical properties decrease. In the case of thermophysical properties, the decrease can be explained by the porous aspect of typha. That is, the progressive presence of typha in the matrices increases the volume of the pores. These result in a decrease in thermal conductivity, thermal effusivity, thermal diffusivity and density. As for mechanical properties, porosity weakens the intermolecular bonds of the matrices due to the increasing presence of typha in the sample, thus explaining this decrease in traction and compression. The results obtained are compared with others found in the literature: we found that the addition of plant fibers decreases the thermophysical and mechanical properties [16-21].

We used these thermophysical results to write the computational codes for the numerical resolution. Therefore, we will present the results and discussions below.

5.2. Numerical Modeling Results and Discussions

5.2.1. Evolution of Temperature as a Function of Depth

Figure 5 below shows the temperature evolution as a function of the depth of the material.

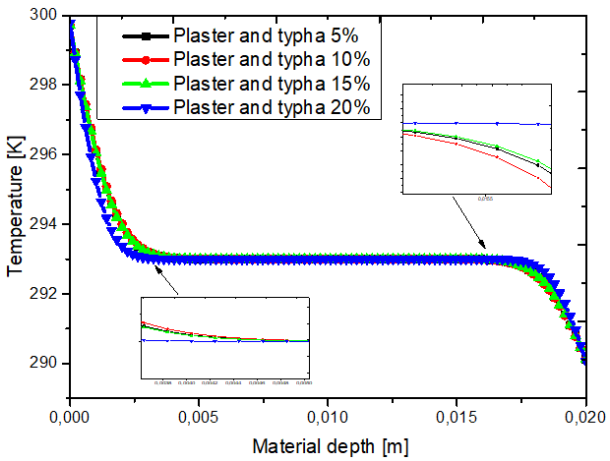

Figure 5. *Temperature versus depth with h1= 30 $W.m^{-2}.K^{-1}$ and h2=10 $W.m^{-2}.K^{-1}$; x=0,02 m.*

In Figure 5, we observe three temperature progressions in the material. Both are identical on the profile side and the rest is linear. For the first phase, the decreasing temperature can be explained by a heat retention of the front face, but arriving at a certain thickness: 0.5 cm, 0.45 cm and 0.32 cm for typha contents of 5%, 10% to 15% and 20% respectively. We reached the linear phase of the different samples for their minimum thermal insulation thicknesses listed above. For the

thickness closer to the back face, we observe the opposite phenomenon; this can be explained by a temperature difference that exists between the two faces. In addition, the fiber content in the matrix influences the dimensions of the thermal insulation thickness. In summary, for a temperature variation of 10°C in samples of 5%, 10% to 15% and 20% in typha. The minimum insulation thicknesses are respectively 1 cm, 0.9 cm and 0.64 cm with values of the exchange coefficient of the front face (h1 =30 $W.m^{-2}.K^{-1}$) and rear (h2 =10 $W.m^{-2}.K^{-1}$).

Figure 5 illustrated the temperature variation as a function of depth for different gypsum binder composites with typha contents. Figures 6, 7, 8 and 9 study the influence of the front panel's heat exchange coefficient on the thickness of the thermal insulation.

5.2.2. Evolution of Temperature as a Function of Depth Under the Influence of the Exchange Coefficient of the Front Face h1

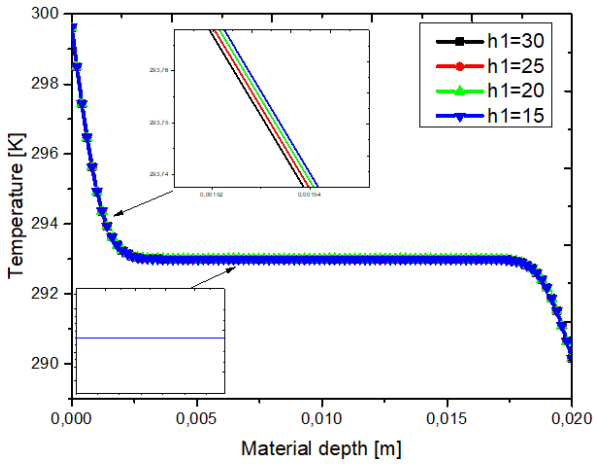

Figure 6. *Temperature versus depth of the composite sample of plaster and 5% typha with the influence of the exchange coefficient h1 and h2=10 $W.m^{-2}.K^{-1}$; x= 0,02 m.*

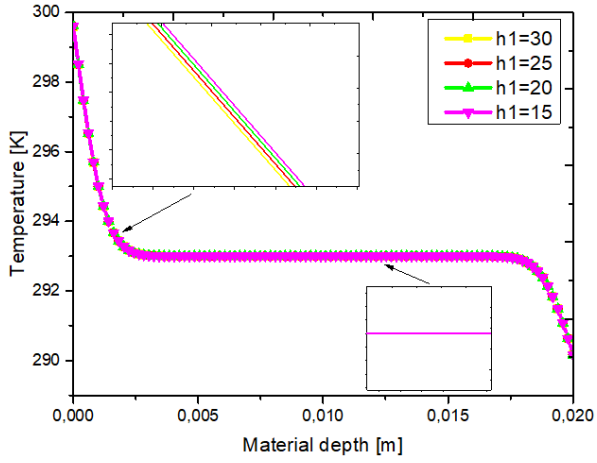

Figure 7. *Temperature versus depth of the composite sample of plaster and 10% typha with the influence of the exchange coefficient h1 and h2=10 $W.m^{-2}.K^{-1}$; x= 0,02 m.*

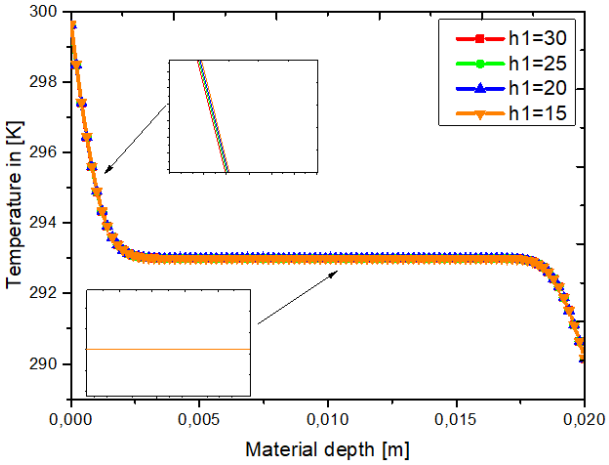

Figure 8. *Temperature versus depth of the composite sample of plaster and 15% typha with the influence of the exchange coefficient h1 and h2=10 $W.m^{-2}.K^{-1}$; x= 0,02 m.*

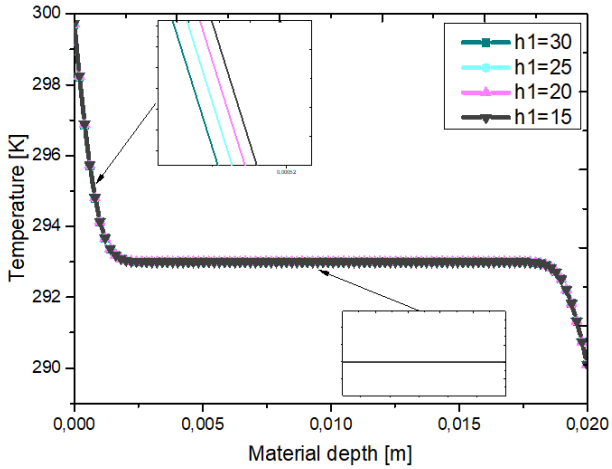

Figure 9. *Temperature versus depth of the composite sample of plaster and 15% typha with the influence of the exchange coefficient h1 and h2=10 $W.m^{-2}.K^{-1}$; x= 0,02 m.*

Figures 6, 7, 8 and 9 show the temperature profile as a function of depth, under the influence of the exchange coefficient of the front face of composites with gradual typha contents.

These curves show the temperature evolution as a function of depth under the influence of the front face heat exchange coefficient of different gypsum binder composites with Typha contents. For these different values of the front face heat exchange coefficient, the temperature profiles are the same for these varying Typha proportions (5%, 10%, 15%, and 20%). However, we found that, for different Typha proportions, these heat exchange coefficient values have a slight influence on the thermal insulation thickness. However, those with the highest coefficient reach the minimum thermal insulation thickness first. In summary, these values (15, 20, 25, and 30 $W.m^{-2}.K^{-1}$) of the front face heat exchange coefficient do not have a significant influence on the thermal insulation thickness.

Figures 6, 7, 8 and 9 show how the heat exchange coefficient of the front face influences temperature variation as a function of depth for these composite materials. Figures 10, 11, 12 and 13 will show the impact of the back face heat exchange coefficient on temperature variation as a function of depth for the different samples.

5.2.3. Evolution of Temperature as a Function of Depth Under the Influence of the Exchange Coefficient of the Front Face h2

Figures 10, 11, 12 and 13 below illustrate the evolution of temperature as a function of depth under the influence of the exchange coefficient of the back face in different composite samples of plaster and typha.

Figures 10, 11, 12 and 13 show the evolution of temperature as a function of depth under the influence of the heat exchange coefficient of the back face in different gypsum-bonded composites with different typha contents. For the different values of the heat exchange coefficient of the back face, the temperature profiles are the same in these different figures with varying Typha proportions (5%, 10%, 15% and 20%). However, we found that, for different Typha proportions, these values of the heat exchange coefficient have no influence on the thermal insulation thickness. This can be explained by the fact that the back face is not exposed to the greatest heat. In short, for these different values of the heat exchange coefficient of the back face (15, 20, 25 and 30 $W.m^{-2}.K^{-1}$), thermal insulation thickness remains constant.

Figures 10, 11, 12 and 13 show the evolution of temperature as a function of depth for plaster-based composite matrices with gradual typha content under the influence of the backside exchange coefficient. Figures 14, 15, 16 and 17 show temperature variation as a function of time for these different composites, highlighting these different values (2.022, 4.044, 6.066 and 8.088) of excitation depth.

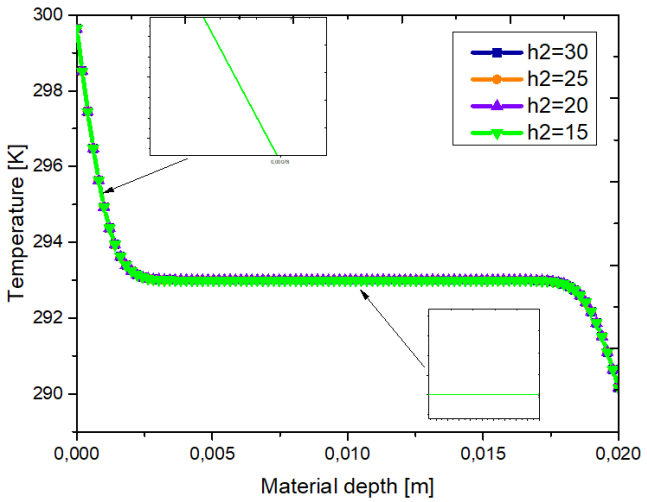

Figure 10. *Temperature versus depth of the composite sample of plaster and 5% typha with the influence of the exchange coefficient h2 and h1=10 $W.m^{-2}.K^{-1}$; x= 0,02 m.*

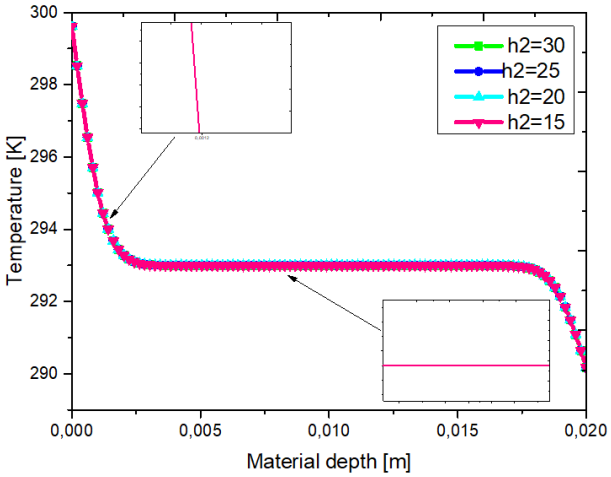

Figure 11. *Temperature versus depth of the composite sample of plaster and 10% typha with the influence of the exchange coefficient h2 and h1=10 $W.m^{-2}.K^{-1}$; x= 0,02 m.*

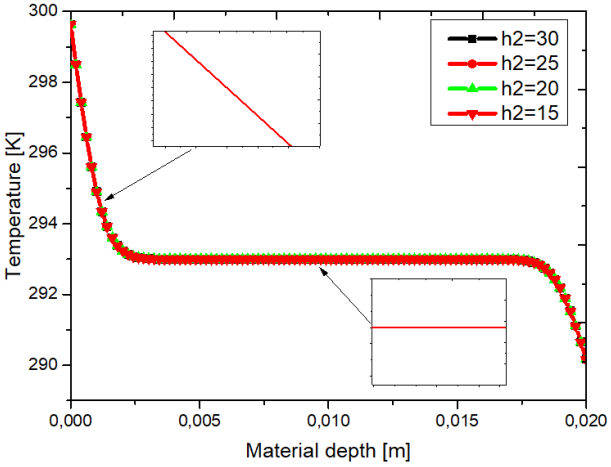

Figure 12. *Temperature versus depth of the composite sample of plaster and 15% typha with the influence of the exchange coefficient h2 and h1=10 $W.m^{-2}.K^{-1}$; x= 0,02 m.*

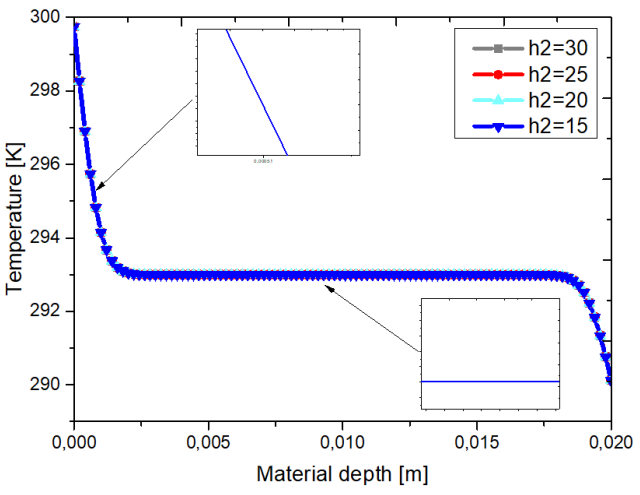

Figure 13. *Temperature versus depth of the composite sample of plaster and 15% typha with the influence of the exchange coefficient h2 and h1=10 $W.m^{-2}.K^{-1}$; x= 0,02 m.*

5.2.4. Evolution of Temperature as a Function of Time

Figures 14, 15, 16 and 17 below show the temperature profile as a function of time, highlighting the depth of excitation.

Figures 14, 15, 16 and 17 show temperature vs. time curves under the influence of excitation depth, with fixed values of the front and rear face exchange coefficients. For these different proportions of typha, we observed the same curves for these different values of the excitation depth. However, for small depth excitations, the material heats up faster than with those of great depths. For times t = 150 s and more, we reached the quasi-static regime for these different exciter depths. This can be explained by the fact that the material heats up before storing heat for the remainder of the excitation. In other words, materials with very small thicknesses are very sensitive to heat.

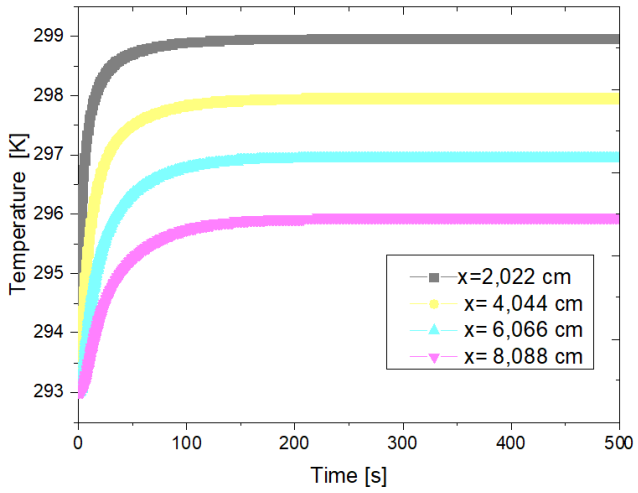

Figure 14. *Temperature versus time for plaster composite and 5% typha.*

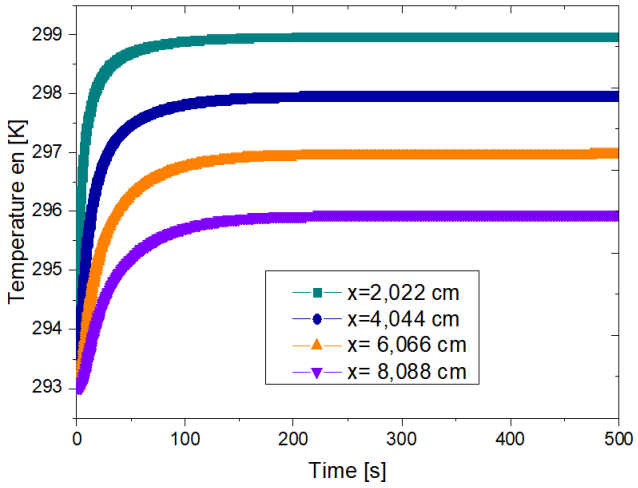

Figure 15. *Temperature versus time for plaster composite and 10% typha.*

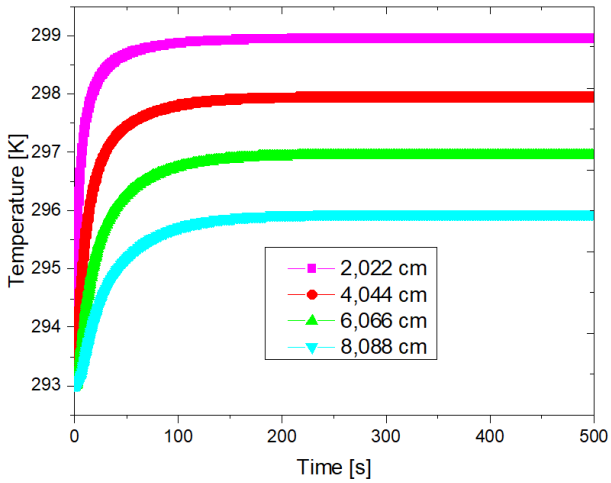

Figure 16. *Temperature versus time for plaster composite and 15% typha.*

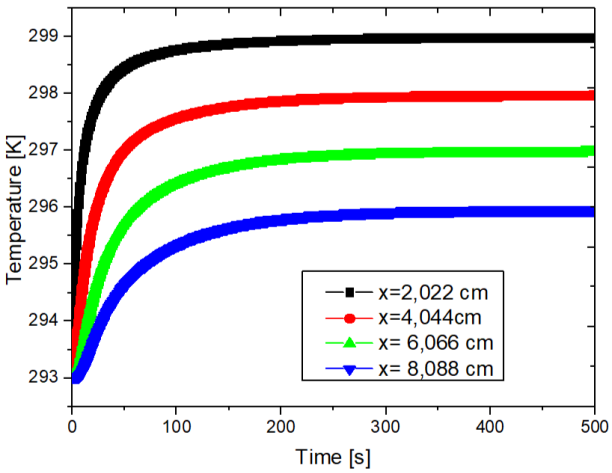

Figure 17. *Temperature versus time for plaster composite and 20% typha.*

Browsing work done by other researchers, the temperature increase as a function of time shows that the material heats up over time [22, 23]. This results in thermal energy storage. Figures 14, 15, 16 and 17 show the temperature evolution over time of plaster binder composites with typha contents, under the influence of excitation depth. The following will summarize the course of the article.

6. Conclusion

The thermomechanical characterization and numerical modeling of heat transfer of plaster-based insulating composite materials with gradual typha contents yielded the following results:

First, the thermophysical and mechanical properties decrease as the mass percentage of typha in the sample increases. These thermophysical results, used for numerical modeling, yielded thermal insulation thicknesses of 1 cm, 0.9 cm, and 0.64 cm with typha contents of 5%, 10% to 15%, and 20%,

respectively, in these plaster binder composite matrices for a temperature varying by approximately 10°C. Then, for a variation in the heat transfer coefficient values of the front face at 15, 20, 25, and 30 with that of the rear face constant. The impact is not very significant on the thermal insulation thickness, but the largest value first reaches the minimum thermal insulation thickness. For these different values of the exchange coefficient of the back face, the insulation thickness remains constant with a fixed value on the front face. Finally, for these different values (2.022, 4.044, 6.066 and 8.088 cm) of the excitation depth, the rates are the same. Materials with small thicknesses heat up faster compared to large depths. In other words, materials heat up as a function of time. before reaching their quasi-static regimes from t=150 s and beyond.

In the future, we plan to study the humidity of materials before implementing them in the construction sector.

Abbreviations

K Kelvin

Conflicts of Interest

The authors declare no conflicts of interest.

References

[1] Global Alliance for Buildings and Construction, «"2020 Global State of Buildings and Construction Report"».

[2] Zheng Lu, Michael Hauschild, Lisbeth M. Ottosen, Teklit Gebregiorgis Ambaye, Pierluigi Zerbino, Davide Aloini, Ana T. Lima, « Climate mitigation potential of biobased insulation materials: A comprehensive review and categorization », Journal of Cleaner Production, volume 470, August 2024, pp. 143356, https://doi.org/10.1016/j.jclepro.2024.143356

[3] Muralikrishnan Alagarsamy, P Pitchipoo, Senthil Kumar, « Comprehensive characterization of spathe fibres extracted from Cocos nucifera: physical, chemical, mechanical, thermal, and acoustic properties for insulation applications», Mater. Res. Express, volume 11, July 2024, pp. 075503.

[4] Lin Chen, Mingyu Yang, Zhonghao Chen, Zhuolin Xie, Lepeng Huang, Ahmed I. Osman, Mohamed Farghali, Malindu Sandanayake, Engui Liu, Yong Han Ahn, Ala'a H. Al-Muhtaseb, David W. Rooney, Pow-Seng Yap, «Conversion of waste into sustainable construction materials: A review of recent developments and prospects», Materials Today Sustainability, volume 27,25 July 2024, pp. 100930, https://doi.org/10.1016/j.mtsust.2024.100930

[5] Sophie Trachte, Dorothée Stiernon, « Balanced choice of thermal insulation during renovation. How to meet energy performance requirements while limiting the overall environmental impact and promoting the circularity of materials," lieuxdits#24, December 2023, pp. 14-21.

[6] Aguerata Kabore, Claudiane M. Ouellet-Plamondon, « Improved insulation with fibres in heavy cob for building walls », Industrial Crops & Products, volume 215, May 2024, pp. 118626, https://doi.org/10.1016/j.indcrop.2024.118626

[7] Henri W. Hounkpatina, Victorin K. Chegnimonhanb, Hagninou E. V. Donnoua, Guy H. Hounguè, Basile B. Kounouhewa, « Thermal characterisation of insulation panels based on vegetable typha domengensis and starch », scientific African, volume 21, 2023, pp. e01786, https://doi.org/10.1016/j.sciaf.2023.e01786

[8] Thibaut Lecompte, «Hemp in the buildings of tomorrow: advantages, constraints and challenges", Annales de Bretagne et des Pays de l'Ouest, online January 4, 2023.

[9] Ahmed Alami, Lala Rajaoarisoa, Nicolas Dujardin, Ali Benouar, Khacem Kaddouri, Khedidja Benouis and Mohammed-Hichem Benzaama, « Artificial Intelligence Approach for Bio-Based Materials' Characterization and Explanation », Buildings, volume, June 2024, pp. 1602, https://doi.org/10.3390/buildings14061602

[10] Basim Abu-Jdayila, Abdel-Hamid Mourad, Waseem Hittini, Muzamil Hassand, Suhaib Hameedi, « Traditional, state-of-the-art and renewable thermal building insulation materials: An overview », Construction and Building Materials, volume 214, 2019, pp. 709–735, https://doi.org/10.1016/j.conbuildmat.2019.04.102

[11] M. S. Ould Brahim, S. Tamba, M. Sarr, A. Diène, I. Diagne, F. Niang et G. Sissoko, «Evolution of the overall thermal exchange coefficients of kapok-plaster and tow-plaster materials in dynamic frequency regime", Revue des Energies Renouvelables, Vol. 14, N°2, 2011, pp. 203 – 210.

[12] J. C. Damfeu, P. Meukama and Y. Jannot, « Modelling and measuring of the thermal properties of insulating vegetable fibers by the asymmetrical hot plate method and the radial flux method: kapok, coconut, groundnut shell fiber and rattan », Thermochimica Acta, volume 630, 2016, pp. 64-77, https://doi.org/10.1016/j.tca.2016.02.007

[13] Younouss Dieye, Vincent Sambou, Mactar Faye, Ababacar Thiama, Mamadou Adj et Dorothe Azilinon, « Thermo-mechanical characterization of a building material based on Typha Australis », Journal of Building Engineering volume 9, 2017, pp. 142-146, https://doi.org/10.1016/j.jobe.2016.12.007

[14] Ibrahima Diaw, Mactar Faye, Stéphane Hans, Frederic Sallet and Vincent Sambou, «Valorization of the Recovered Lime in Cement-Typha Concretes: Thermal and Mechanical Behavior», InterSol 2022, LNICST, volume 449, February 2023, pp. 267–276 76, https://doi.org/10.1007/978-3-031-23116-2_23

[15] El Hadji Abdoul Aziz CISSE, Papa Touty Traore, Alphousseyni GHABO, Mor Ndiaye, Issa Diagne, «Thermomechanical characterization of laterite matrix reinforced with typha material for thermal insulation in building », Materials Sciences and Applications, volume 15, 2024, pp. 450-463, https://doi.org/10.4236/msa.2024.1510030

[16] Harouna Bal, Yves Jannot, Salif Gaye, Frank Demeurie, «Measurement and modelisation of the thermal conductivity of a wet composite porous medium: Laterite based bricks with millet waste additive», Construction and Building Materials volume 41, January 2013, pp. 586–593, https://doi.org/10.1016/j.conbuildmat.2012.12.032

[17] Nadia Benmansour, Boudjemaa Agoudjil, Abdelkader Gherabli, Abdelhak Kareche, Aberrahim Boudenne, «Thermal and mechanical performance of natural mortar reinforced with date palm fibers for use as insulating materials in building», Energy and Buildings volume 81, June 2014, pp. 98–104, https://doi.org/10.1016/j.enbuild.2014.05.032

[18] Sibiath O. G. OSSENI, Berléo D. APOVO, Clément AHOUANNOU, Emile A. SANYA et Yves JANNOT, «Thermal characterization of cement mortars doped with coconut fibers by the asymmetric hot plane method at a temperature measurement», Afrique SCIENCE, volume 12, n°6, 2016, pp. 119 – 129.

[19] Harouna Bal, Yves Jannot, Nathan Quenette, Alain Chenu, Salif Gaye, «Water content dependence of the porosity, density and thermal capacity of laterite-based bricks with millet waste additive», Construction and Building Materials, volume 31, January 2012, pp. 144–150, https://doi.org/10.1016/j.conbuildmat.2011.12.063

[20] Yoann Brouard, Naima Belayachi, Dashnor Hoxha, Narayanaswami Ranganathan, Stéphane Méo, «Mechanical and hygrothermal behavior of clay – Sunflower (Helianthus annuus) and rape straw (Brassica napus) plaster bio-composites for building insulation», Construction and Building Materials, volume 161, 2018, pp. 196–207.

[21] A. Laborel-Préneron, J-E. Aubert, C. Magniont, A. Bertron, «Influence of straw content on the mechanical and thermal properties of bio-based earth composites», First International Conference on Bio-based Building Materials, 22 – 24 June 2015, Clermont-Ferrand, France.

[22] Seydou FAYE, Papa Touty TRAORE and Babou DIONE, «Study in Transient Regime by Analytical Method of Heat Transfer through a Kapok-plaster Insulating Material has one Dimension: Influence of the Heat Exchange Coefficient», Journal of Scientific and Engineering Research, volume 8, n°9, 2021, pp. 199-206.

[23] Mamadou Babacar Ndiaye, Ahmadou Diop, Seydou Faye, Youssou Traore and Gregoire Sissoko, «Study of a flat panel based on typha and clay in transient regime», Int. J. Adv. Res. Volume 8, n°12, December 2020, pp. 751-758.